Published in Physical Chemistry Chemical Physics 13: 20939-20945, 2011

Disentanglement of triplet and singlet states of azobenzene: direct EELS detection and QMC modeling

M. Dubecký,[a] R. Derian,[a] L. Horváthová,[a] M. Allan[b] and I. Štich*[a]

Singlet and triplet excited states of *trans*-azobenzene have been measured in the gas phase by electron energy loss spectroscopy (EELS). In order to interpret the strongly overlapping singlet and triplet bands in the spectra a set of large-scale correlated quantum Monte-Carlo (QMC) simulations was performed. The EELS/QMC combination of methods yields an excellent agreement between theory and experiment and for the two low-lying excited singlet and two low-lying triplet states permitted their unambiguous assignment. In addition, EELS revealed two overlapping electronic states in the band commonly assigned as S_2, the lower one with a pronounced vibrational structure, the upper one structureless. Finally, the agreement between theory and experiment was shown to further increase by taking computationally into account the finite temperature effects.

I. Introduction

Azobenzene (AB), $C_{12}H_{10}N_2$, is perhaps the most prominent photoswitchable molecule with a relatively simple molecular structure. AB exists in the two structural isomers shown in Fig. 1, the energetically more stable *trans* (*E*) isomer and the metastable *cis* (*Z*) isomer, which have different physical, electronic, and transport properties.[1,2] The *E* isomer is markedly longer compared to the *Z* isomer, by ~2.4 Å, and has a dramatically higher conductance, by two orders of magnitude, with respect to the *Z* isomer.[3] Laser light of appropriate wave length[1,2] induces $E \rightleftharpoons Z$ photoswitching in AB. In the ground state, S_0, $Z \rightarrow E$ isomerization can take place also thermally.[1,2] The two isomers exhibit different absorption bands which make AB a good candidate for light-triggered switches, image storage devices, and materials with photo-modulable properties.[1,2] The isomerization is generally tacitly assumed to proceed in the singlet state. As shown below, triplet states can be involved and play an important role in thermal isomerization. The neglect of the role of the triplet states is presumably in part a consequence of the scarcity of experimental studies of the triplet states—existing experiments reported only absorption into singlet states.[4–7] The main goal of this manuscript is to fill the gap and to provide the most complete characterization of the electronic structure of AB by a joint experimental/theory study.

[a] *Institute of Physics, Center for Computational Materials Science, Slovak Academy of Sciences, 84511 Bratislava, Slovakia. E-mail: ivan.stich@savba.sk*
[b] *Department of Chemistry, University of Fribourg, chemin du Musée 9, 1700 Fribourg, Switzerland*

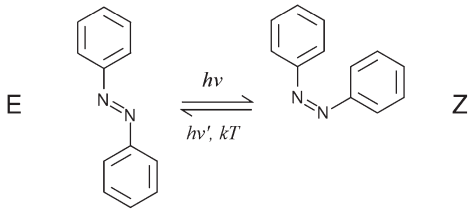

Fig. 1 Structure of *trans* (*E*) and *cis* (*Z*) isomers of azobenzene featuring different CNNC dihedral angles.

Low-energy absorption spectra of AB have been measured for both isomers in gas phase[4] and inert solvents.[5–7] They show peaks attributed to the lowest $n\pi^*$ (S_1) and $\pi\pi^*$ (S_2) singlet states. The experiments were performed at temperatures from room temperature[8] to temperatures in excess of 500 K,[4] in some cases different parts of the same spectra were measured at different temperatures.[4]

Experimental information on low-energy triplet states (T_1, T_2, ...) of AB is scarce, despite the fact that the $S_0 \rightarrow T_1$ spin–orbit coupling is an order of magnitude larger than values typical for aromatic compounds.[9] No phosphorescence spectrum has been detected to date, and absorption spectra failed to reveal any band attributable to the singlet–triplet absorption or to triplet–triplet transient absorption upon laser excitation. To the best of our knowledge to date only two brief reports on triplet states of AB exist. Shashoua[10] attributed to T_1 a state at ~2.3 eV determined by magneto-optical rotary dispersion. Indirect information on T_1 was obtained by Monti *et al.* by analyzing the rate constant for energy transfer from a number of energy donors with different triplet energies.[11] Adiabatic energies of 1.52 eV and 1.78 eV were determined for the T_1 states of the *E* and *Z* isomers, respectively. The fact that so far the T_1 state escaped direct

observation points to its very short lifetime.[12] DFT calculation revealed a T_1 state at the energy of 1.48 eV.[12] Using CAS-SCF/CAS-PT2 techniques this energy was later refined to 1.83 eV.[9] Four triplet states were calculated by Hättig and Hald[13] using the CC2 and CCSD methods. However, as we show below, these computed energies vary considerably with the method used as do those calculated for singlets. These facts indicate that despite numerous experimental[4–8,10,11] and theoretical[9,12–24] studies, photochemistry of AB is far from adequately understood, both in terms of availability of complete and accurate spectral data and of theoretical description of the quantum effects involved.

In this paper we fill the gap in our understanding of the photochemistry of AB by presenting fully correlated *quantum Monte Carlo* (QMC)[25,26] simulations, transcending our previous study of the lowest singlet states (S_0, S_1)[24] to a higher singlet state (S_2) and adding triplet states (T_1, T_2, ...), and by validating the theoretical predictions by comparison with electron energy loss (EEL) spectra of gas phase *trans* AB taken at a range of residual electron energies permitting the observation of both singlet and triplet states.

The QMC method is superior for the present task because short-range correlations are treated exactly and do not limit the accuracy of the results. The present calculations are a formidable task, as we deal with *ground- and excited states* of a large molecule with almost hundred electrons deemed until recently beyond practical computational feasibility. Due to its favorable low-order polynomial scaling with the system size,[25,26] the QMC method provides a practical route to achieving chemical accuracy ($\sim$0.04 eV) for this system. In addition, we use a combination of different methods to provide lower bound estimates of thermal effects which affect the experimental spectra. Our final QMC results reduce residual errors to $\sim$0.1 eV, an outstanding achievement for a system of this size. The accuracy is enough to provide guidance in disentangling the host of overlapping singlet and triplet bands in the EEL spectra and in understanding the photochemistry of AB.

Concerning alternatives to QMC, the simplest approach is based on the DFT and generalized restricted open shell Kohn–Sham (gROKS) description of the lowest excited singlet state S_1[14–17] and triplet state T_1.[12] The best quantum chemistry results up to date use CC2,[13,18] CCSD,[13] and CAS-SCF/CAS-PT2 description.[9,12,19] While the use of these methods allows exploration of the potential hypersurface and thus provides very useful insights into dynamics of AB[14–17,20] or possible conical intersections, photo-isomerization pathways, quantum yields, *etc.*,[9,12,19,22,23] the insufficient accuracy of electronic correlation treatments by all these methods significantly limits the predictive power of the results. In contrast, the accuracy of the QMC method is limited only by the accuracy of the nodal hypersurfaces of the trial many-body wave function, fixed by CAS-SCF wave function in present simulations.[24] Short-range correlations, treated only perturbatively at the CAS-PT2 level, are exact in QMC. Most of the QMC applications up to date are restricted to ground states of fairly small molecular systems, with excited states still representing a direction with fairly little expertise.[27–30] Only recently truly large-scale QMC photochemical calculations started to appear.[24,31–33]

The main initial goal of this study was to shed light on the low-energy triplet states of *trans* AB by a joint experimental/theory study. In doing so we revealed complete electronic structure of *trans* AB, including also singlets where new gas phase results are also needed. In particular, we unambiguously assign the first two triplet and singlet states, identify three higher-lying triplet states and a host of singlet and triplet states in the 6–8 eV range. The accurate correlated QMC simulations turned out indispensable in disentanglement of the triplet and singlet states and in understanding the measured EEL spectra.

II. Methods

A. Experiment

The trochoidal electron spectrometer used in the present study was described in detail previously.[34] It uses magnetic collimation of the electron beams, trochoidal monochromators as electron energy filters, and a collision chamber with small apertures for the incident and scattered electron beams. The experiment involves intercepting the sample vapor at low pressure ($\sim 10^{-4}$ mbar) with a beam of electrons of varying incident energy E_i and detecting electrons scattered at a fixed residual energy E_r. The incident electrons can excite the target molecules, thereby loosing an amount of kinetic energy $\Delta E = E_i - E_r$ equal to the excitation energy. A spectrum of excited states is obtained by plotting the scattered electron current I_s against the electron energy loss ΔE. The collision chamber was kept at about 80 °C during the measurement, the resolution was about 0.05 eV. The energy scale, calibrated on high vibrational overtones of N_2 in AB/N_2 mixtures, is accurate to within 0.03 eV. This instrument detects electrons scattered into forward (0°) and backward (180°) directions.[35] Forward scattering dominates and dipole selection rules apply approximately at $E_r = 20$ eV—the spectrum recorded with $E_r = 20$ eV is consequently similar to the UV/VIS absorption spectrum. Triplet bands appear in the spectra recorded with low residual energies, but the dipole allowed bands do not completely disappear. The cross sections for excitation of the triplet states are often backward peaked, so that the capacity of the present instrument to detect the backward scattered electrons is very helpful for the detection of the triplet states.[35] Spin allowed but dipole forbidden transitions may also appear in the spectra recorded with low E_r.

B. Theory

Simulation of the excitation energies used a five-level modeling: (1) geometry was obtained from DFT optimization, (2) trial wave function was constructed from a truncated CAS-SCF expansion, (3) trial wave function was optimized using VMC (variational Monte-Carlo) techniques, (4) excitation energies were computed from DMC (diffusion Monte-Carlo) simulation, and (5) *ab initio* Car–Parrinello dynamics simulations[36] at various temperatures were used to estimate the finite temperature corrections for various transitions. For static DFT and CAS-SCF we used the GAMESS suite of codes,[37,38] all VMC and DMC calculations used the QWalk code,[39] while for dynamical DFT simulations we used the CPMD planewave pseudopotential code.[40]

As in the EELS experiment, vertical excitation energies were calculated for the *trans* isomer, with the exception of the lowest singlet states, where energies along the torsion

coordinate (CNNC dihedral angle), including barrier heights, were calculated. The reason is that rotation along the CNNC dihedral angle is the preferred pathway for both photo and thermal isomerization processes.[9,19] The ground-state geometries were calculated using DFT techniques with B3LYP exchange-correlation functional[41] with the Greeff–Lester type effective core pseudopotential[42,43] for all species and cc-pVTZ basis set.[44] The use of DFT-optimized ground-state atomic structure in QMC-determined energies may lead to bias. Nevertheless for the *E* isomer, where electron diffraction experiments exist, our B3LYP geometry lies within experimental error bars of the most recent gas-phase electron diffraction experiment.[45] Importance of geometry on the excitation energies of AB has been emphasized by Hättig and Hald,[13] who found effects of 0.2–1.0 eV, depending on the state. The balanced active space in singlet CAS-SCF calculations consisted of 14 electrons in 12 orbitals (14/12)[9,12,19,24] initially constructed from DFT orbitals.[24] In some tests a (16/14) orbital space was used. For the triplets the orbital space was (14/14) constructed from state-averaged CISD calculations.

The natural orbitals and expansion coefficients were generated from CAS-SCF calculations, with orbital space optimized for each state. Subsequently a truncated CAS-SCF expansion was used retaining all symmetry adapted configuration state functions (CSFs) with weights ≥ 0.01 optimized together with variational parameters of the spin-dependent Schmidt–Moskowitz Jastrow correlation factor[26,46] including electron–electron, electron–nucleus, and electron–electron–nucleus terms. The expansions consist of between 107 and 1228 Slater determinants or 38 and 322 CSFs. In VMC, the trial wave functions[26] and their nodes were optimized by minimizing a linear combination of energy and variance.[47] Final results were obtained by DMC runs. In order to estimate thermal corrections, see Section III, we ran finite temperature (300 to 500 K) dynamics simulations $\sim$50 ps long.

The selection of states for the VMC/DMC simulation was based on the CAS-SCF energies. However, as discussed in Section III, dynamical correlations, absent at the CAS-SCF level, often change the ordering of states in energy, causing shifts in energy between states of $\sim$1 eV. In total the first three CAS singlet and the first five CAS triplet states were considered for further QMC treatment. Due to the energy shifts such a procedure does not necessarily yield the lowest energy states. These triplet states are labeled T_m, T_n, T_l.

III. Results and discussion

Fig. 2 shows the EEL spectra as they were recorded. The interpretation of these spectra is hampered by the fact that dipole-allowed and forbidden transitions overlap in the spectra recorded at low E_r, and by the overlap of the triplet bands. In addition, a background due to excitation of a quasicontinuum of high vibrational overtones occurs at low energy-losses, particularly at low E_r.[34]

To facilitate the interpretation we therefore processed the spectra as shown in Fig. 3. First, the low energy-loss background was fitted to the tail of a broad Gaussian profile centered near $\Delta E = 0$ eV and subtracted to obtain a flat baseline below the lowest electronically excited states. The $E_r = 20$ eV spectrum

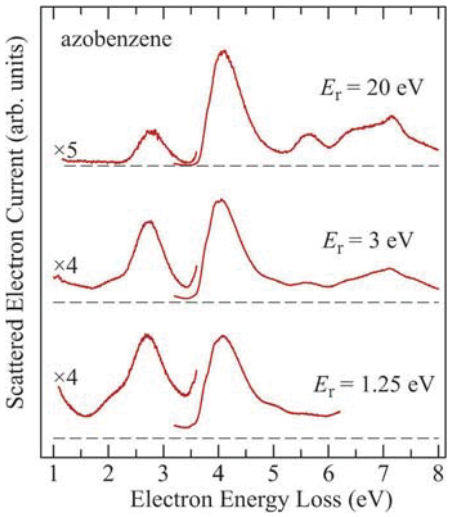

Fig. 2 Raw EEL spectra.

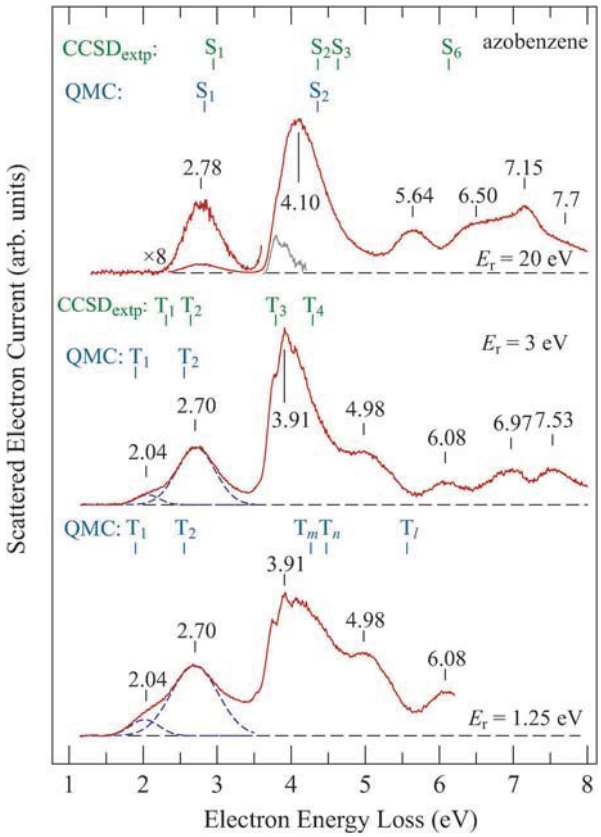

Fig. 3 EEL spectra (red curves) from Fig. 2, processed as explained in the text to improve the visibility of forbidden transitions. Gaussians used to fit the lowest two triplet states are shown by dashed (blue) lines. The results of the present calculations are labeled "QMC", the marks labeled "CCSD$_{extp}$" indicate the "CCSD extrapolated" theory of Hättig and Hald[13] (without the S_4 and S_5 states which have zero oscillator strength).

in the top panel is now very similar to gas-phase VIS/UV absorption spectra and characteristic for dipole-allowed transitions. To obtain spectra of the forbidden transitions, we then subtracted the $E_r = 20$ eV spectrum from the $E_r = 3$ eV

and the E_r = 1.25 eV spectra, multiplying it first by a factor chosen to make the 5.64 eV band, which must be due to an allowed transition, disappear in the difference spectra.

The transition energies (the 2.78, 4.10 and 5.64 eV bands) and the general shape of the spectrum recorded with E_r = 20 eV agree well with published gas phase absorption spectra.[4,48] The only difference is that the S_1 band is only 18× weaker than the 4.10 eV band, whereas in the quantitative absorption spectra it is about 60× weaker.[4,48] This is because the residual energy of E_r = 20 eV is still too low for the high energy limit where the dipole transition intensities apply, and the nominally dipole-forbidden transition to the S_1 state is consequently enhanced. Like in the absorption spectra, the 4.10 eV band has a faint structure, assigned to the N=N stretch vibration—it appears weaker in the EEL spectra because of the inferior resolution. Its visibility is improved in the small (gray) insert under the 4.10 eV band of the E_r = 20 eV spectrum, obtained by subtracting an arbitrary smooth background from the experimental 4.10 eV band. The resolution of EELS is not sufficient to resolve the 220 cm^{-1} structure observed in the absorption spectra.[4]

The 4.10 eV band has a profoundly different shape in the spectrum with E_r = 3 eV in Fig. 3. The low-energy part is strongly enhanced and appears as a band with clear vibrational structures at 3.77, 3.91 and 4.06 eV, *i.e.*, with an average spacing of 0.145 eV (1170 ± 200 cm^{-1}, presumably N=N stretch). Similar observation is made in the E_r = 1.25 eV spectrum. This means that the 4.10 eV band corresponds to two electronic states, one structured peaking at 3.91 eV, the other structureless, peaking at 4.10 eV. It is unlikely that the 3.91 eV band is due to a triplet state, because the same vibrational structure appears also in the E_r = 20 eV EEL and the UV absorption spectra where triplet states are not visible. The observation of two states within the 4 eV band is consistent with the relatively recent evidence of two different decay times (170 and 420 fs) reported across the 4.10 eV band, interpreted as lifetimes of partly overlapping S_2 and $S_{3,4}$ states,[20] and with theoretical predictions.[13,18–20] There is a subtle point, however. It is the 3.91 eV band which is enhanced at low E_r in the present experiment, indicating a higher degree of 'forbiddeness' than the 4.10 eV band. In contrast, the calculations[18] indicate the largest oscillator strength (0.85) for the lowest (S_2) of the three overlapping states, whereas S_3 has an oscillator strength of only 0.02, and S_4 is dark. This represents an indication that the S_2, S_3 ordering may be reversed. This is why we compare the 4.10 eV band, and not the 3.91 eV band, to the calculated S_2 energy. The evidence is not very strong, however, because the calculated oscillator strength of the S_3 (S_4 in ref. 20) is reported to strongly depend on geometry and varies with the theoretical model.[18,20] The EEL spectrum recorded with E_r = 1.25 eV has a very weak narrow shoulder at around 3.55 eV, which is probably a 'hot band' of the 3.91 eV band.

The two low-lying triplet bands overlap and were fitted to Gaussian profiles to determine the peak positions. The fit is only approximate because the experimental Franck-Condon profile is slightly asymmetrical (the high energy side is more gradual than the onset), and because the fitting Gaussian profiles are slightly wider and shifted (by −0.04 and −0.02 eV for T_1 and T_2, respectively) in the E_r = 1.25 eV spectrum when compared to the E_r = 3 eV spectrum. The average values are given in Fig. 3 and the shifts are absorbed in the confidence limit which is taken as ±0.05 eV. The shifts are likely to be a consequence of resonant excitation, whereby the incident electron can, at a suitable incident energy, be trapped in the vicinity of the target molecule for a short time (shorter than a vibrational period), and the positions of the nuclei relax slightly during the lifetime of this "negative ion resonance". The consequence of the relaxation is a small deviation from the Franck-Condon profile. The resonance is more likely to affect the lower E_r spectrum. Finally, the 4.2–4.8 eV spectral region is more "filled" in the E_r = 1.25 eV spectrum than in the E_r = 3 eV spectrum and we interpret this as an evidence for two higher-lying triplet states. Their energies are only estimated to be around 4.3 and 4.6 eV.

We now proceed to comparison of our experimental transition energies derived from the EEL spectra as described above to the QMC theory and to other experiments. In Table 1 results of the present experiment are compared to gas phase absorption experiment,[4] selected previous calculations,[9,12,13,16,17,19,24] and with the present QMC theory. Validation of QMC potential energy surface (PES) in S_0 and S_1 along the CNNC dihedral angle as well as of the transition energies against present and previous[4] gas phase experiments is shown in Fig. 4. For completeness and direct comparison the present QMC results and results of the "CCSD extrapolated" calculation of ref. 13 are also shown graphically in the EEL spectra in Fig. 3.

Both Table 1 and Fig. 3 indicate a very good agreement of the present QMC results with the experimental values for the T_1, S_1, T_2, and S_2 states. The most important novel information from our QMC calculation comes from the study of triplet states. We confirm the presence of the T_1 state by computationally locating it at 1.89 eV, which agrees nicely with the experimental shoulder position at 2.04 eV. Other calculations find T_1 at energies spread between 1.48 and 2.4 eV[9,12,13] depending on the method used. Our calculated value of 2.55 eV for the T_2 state compares favorably with the experimental value of 2.70 eV. The earlier theoretical study, the CC2/CCSD calculations,[13] yielded energies of 1.75 eV (CCSD), 2.83 eV (CC2), and 2.64 ($CCSD_{extp}$)—see Table 1.

The calculated T_m and T_n energies are also well consistent with the EEL spectrum recorded with E_r = 1.25 eV, although an accurate comparison is not possible because of severe band overlap in the experimental spectrum. More precise assignment of these states is hampered by the fact that the CAS wave functions provide a poor initial guess for QMC, see Fig. 5 for more details. More triplet states at energies around of ∼4 eV are expected theoretically, but cannot be assigned by our current computation, as more CAS states would have to be considered because of massive energy shifts due to dynamical correlation. We therefore do not assign any specific values to the indexes m, n, l in T_m, T_n, and T_l in Table 1.

The first state above S_2 having an appreciable oscillator strength is calculated to be S_6[13,18] and we assign it to the 5.64 eV EEL and UV bands. It appears substantially too high in the "CCSD extrapolated" calculation shown in Table 1, but other calculations place it closer to the observed value. Its photochemistry has recently been studied (at 6 eV) and found to yield excitation-specific photochemistry with C–N bond scission instead of isomerization.[49]

Table 1 Vertical excitation energies from the $S_0(^1A_g)$ ground state to various singlet and triplet final states for the *trans* isomer of AB, energy differences between the ground states of the *E* and *Z* isomers $\Delta E_{S_0}^{E-Z}$, and energies of the transition state on the S_0 (T_1) surface $\Delta E_{S_0}^{TS}$ ($\Delta E_{T_1}^{TS}$). Values calculated using various methods and experimental results are compared for all quantities. All energies are in eV, relative to the *E* isomer. The experimental data are, when not otherwise noted, the present results, with a confidence limit of ±0.05 eV

Final state	DFT[b]/gROKS[c]	CCSD[d]	RI-CC2[e]	$CCSD_{extp}$	CAS-SCF[b]	CAS-PT2[b]	DMC	Expt.	
$S_1(^1B_g)$ ($n\pi^*$)	2.17[i,j]	2.94[l]	2.84[l]	2.95[l]	3.18[m,n]	2.53[m,n]	2.82(6)[o]	2.78	2.82[p]
$S_2(^1B_u)$ ($\pi\pi^*$)	—	3.85[l]	4.04[l]	4.36[l]	6.35[m,n]	4.23[m,n]	4.35(6)/4.23(6)[h]	4.10	4.12[p]
$S_3(^1B_u)$ ($\pi\pi^*$)	—	4.31[l]	4.44[l]	4.63[l]	5.71[m,n]	4.46[m,n]	—	3.91[g]	—
⋮									
$S_6(^1B_u)$ ($\pi\pi^*$)	—	5.85[l]	5.79[l]	6.13[l]	—	—	—	5.64	5.64[p]
$T_1(^3B_g)$ ($n\pi^*$)	1.48[f,k]	2.21[l]	2.26[l]	2.31[l]	1.73[f,m,n]	1.83[f,m,n]	1.89(6)	2.04	—
$T_2(^3B_u)$ ($\pi\pi^*$)	—	1.75[l]	2.83[l]	2.64[l]	—	—	2.55(5)	2.70	—
⋮									
$T_m(^3A_g)$ ($\pi\pi^*$)	—	3.62[l]	4.03[l]	3.79[l]	—	—	4.26(5)	~4.3	—
$T_n(^3B_u)$ ($2\pi\pi^*$)	—	4.03[l]	4.24[l]	4.29[l]	—	—	4.47(5)	~4.6	—
$T_l(^3A_g)$ ($2\pi\pi^*$)	—	—	—	—	—	—	5.49(5)	—	—
$\Delta E_{T_1}^{TS}$	—	—	—	—	—	—	1.40(6)[f,o]	—	—
$\Delta E_{S_0}^{TS}$	1.73[i,j]	—	—	—	1.80[m,n]	1.65[m,n]	1.80(6)[o]	—	1.73[a,p]
$\Delta E_{S_0}^{E-Z}$	0.51[i,j]	—	—	—	0.71[m,n]	0.52[m,n]	0.50(6)[o]	—	0.55[p]

[a] Assuming $\Delta E_{S_0}^{E-Z} = 0.51$ eV.[8] [b] 6-31G* basis. [c] Plane-wave basis. [d] cc-pVTZ basis. [e] aug-cc-pVTZ basis. [f] Adiabatic. [g] Ordering uncertain, see text. [h] After finite temperature correction. [i] Ref. 16. [j] Ref. 17. [k] Ref. 12. [l] Ref. 13. [m] Ref. 9. [n] Ref. 19. [o] Ref. 24. [p] Ref. 4.

Finally we wish to discuss the relation of our QMC results with those from other theoretical models. As the results represent excitations from ground state S_0 PES we start by discussing the quality of description of the S_0 surface along the CNNC dihedral angle. We find, see Table 1, that all methods, except for CAS-SCF, describe well the energy difference $\Delta E_{S_0}^{E-Z}$ between the minima corresponding to *trans* and *cis* isomers. At the barrier ($\Delta E_{S_0}^{TS}$) this PES involves a complicated state formed by cleavage of a π-bond in the N=N group to form a biradical intermediate and correspondingly the computed barrier height varies between 1.65 (CAS-PT2) and 1.80 eV (DMC). The DMC barrier $\Delta E_{S_0}^{TS}$ shows only a marginal difference of ~0.07 eV compared to the gas phase experiment.[4] There are two possible sources for this difference. In our calculations the transition state has been fixed to a dihedral angle of 90°, whereas the real value may be slightly different. More importantly, a non-adiabatic $S_0 \rightarrow T_1 \rightarrow S_0$ torsion pathway *via* the first excited triplet state, T_1, which crosses the S_0 PES, was proposed,[9,19] consistent with large $S_0 \rightleftharpoons T_1$ spin–orbit coupling found for AB.[9] Indeed, our T_1 DMC adiabatic energy of 1.40 eV computed at the transition state, $\Delta E_{T_1}^{TS}$, corroborates this scenario.

Substantial differences are found between the various theoretical methods for excited state energies. The gROKS method underestimates the S_1 excitations by as much as ~0.7 eV,[16,17] CAS-SCF results[9,19] significantly overestimates the excitations by ~0.4 eV, while CAS-PT2 results[9,19] underestimates the excitations by up to 0.3 eV with respect to the gas phase experiments. A somewhat better estimate is provided by the $CCSD_{extp}$,[13] overestimating the S_1 excitation by ~0.2 eV. The *accuracy* achieved with QMC methods can clearly be seen in Table 1 and Fig. 4. Most of the studied transitions are either symmetry or spin forbidden. The exception being $S_0 \rightarrow S_2$, which is indeed dominating the EEL spectrum in the top panel of Fig. 3. Our estimated oscillator strength of this transition at the CAS-SCF level is 0.84. The DMC energy of $S_0 \rightarrow S_2$ of

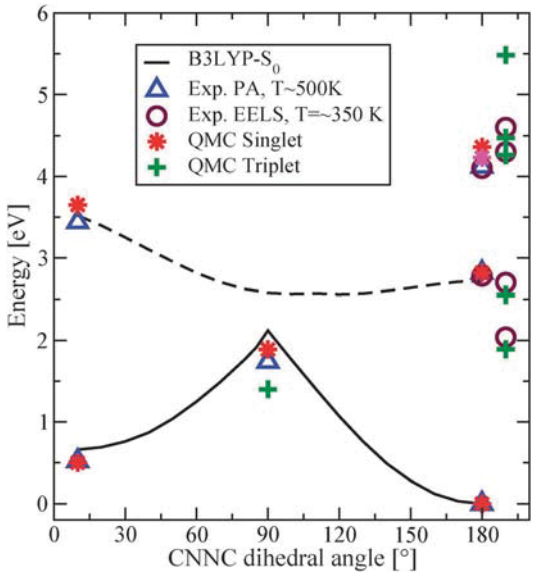

Fig. 4 Computed singlet and triplet vertical excitation energies compared to results inferred from EEL spectra and previous photoabsorption (PA) experiment.[4] For ground-state, S_0, results along the torsion pathway are shown along with experimental results[4] and results of previous calculation.[24] At the barrier the adiabatic T_1 energy is also shown because it is presumed to be important for thermal isomerization *via* the non-adiabatic torsion route involving $S_0 \rightarrow T_1 \rightarrow S_0$ crossing. The dashed line is a guide to the eye roughly corresponding to the S_1 surface.[24] For the S_2 state, the temperature corrected QMC energy is shown in magenta. In QMC results error bars are smaller than the size of the points. All energies are in eV, relative to the *E* conformer.

4.35 eV appears to be higher than both experimental values of 4.10 and 4.12 eV,[4] where the CAS-PT2 result of 4.23 eV appears to be in better agreement with experiments. However, $CCSD_{extp}$[13] yields an excitation energy very similar to our QMC result. To test the robustness of our results we have enlarged our orbital space in constructing the trial wave function to (16/14) to arrive at exactly the same excitation

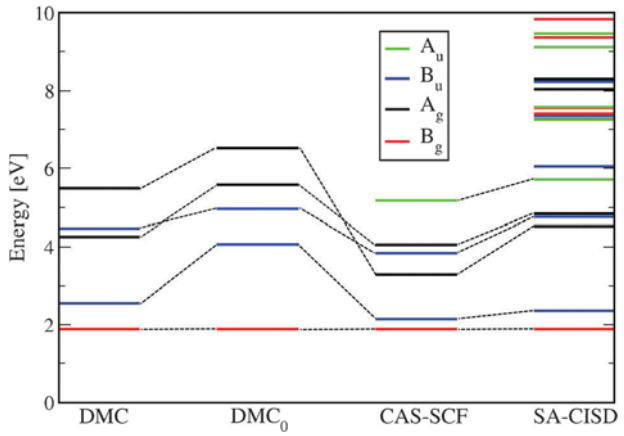

Fig. 5 Energy ordering of the triplet states considered at different stages of optimization. Color coding corresponds to different representations of the final state in C_{2h} symmetry point group. From right to left: SA-CISD (state averaged configuration interaction with single and double excitations), CAS-SCF, DMC_0 (DMC energy with CAS-SCF nodal hypersurfaces without further VMC optimization), and DMC. All energies are aligned to the DMC energy of T_1. Final DMC energies correspond to T_1, T_2, T_m, T_n, and T_l states; for details see the text.

energy of 4.35 eV. We argue below that the agreement with experiments improves by inclusion of thermal effects.

As for triplets, our QMC estimate of the T_1 is in much better agreement with the experiment than the CC2/CCSD predictions[13] and in slightly better agreement than CAS-PT2.[9,19] CCSD estimate of T_2 energies[13] clearly demonstrates the basis set dependence of the traditional quantum chemistry methods. At the aug-cc-pVTZ level, CCSD yields a wrong ordering of the energies which is only corrected in $CCSD_{extp}$ after basis set effect correction.[13] Our DMC energies are free of such an error, as they use δ-functions as a basis set. QMC estimates of the excitation energies of the higher triplet states are also in better agreement with experiments than the CC2/CCSD energies.[13]

We investigated the question whether the remaining difference between the DMC and the experimental transition energies could be, at least in part, due to *temperature effects*. The experiment measures excitation energies averaged over a range of configurations which the target molecule can reach thermally. In contrast, the theoretical excitation energies are computed for a single (ground-state) optimized geometry. In order to provide results more directly comparable to the measured values, the excitation energies would have to be sampled along a finite-temperature trajectory. In a preliminary study we attempted to estimate the finite temperate effects by taking into account the CNNC dihedral angle distribution sampled at the S_0 DFT PES by Car–Parrinello dynamics using the somewhat cheaper CAS-PT2 energies to estimate the excitation energies. This yielded a prediction that the finite temperature corrected transition energies at 500 K should be lower than the vertical values by 0.12, 0.02, and 0.01 eV for the S_2, S_1, and T_1 states, respectively, thus improving the agreement between QMC theory and experiment, in particular for the S_2 state where the difference is currently the largest. Adding finite temperature corrections also to the other transitions and/or extending the model beyond the CNNC dihedral is expected to further improve the agreement with experiment.

IV. Conclusions

We present a complete electronic structure measurement of *trans*-azobenzene in the gas phase, including both singlet and triplet excited states, by electron energy loss spectroscopy (EELS) supported by a set of large-scale correlated quantum Monte-Carlo (QMC) simulations. The calculated *vertical excitation energies into the lowest two singlet and triplet states* are in excellent agreement with the energies of the band maxima in the EEL spectra, the differences being −0.14 eV for the T_1 and T_2 states, and 0.04 eV and 0.25 eV (0.13 eV after finite temperature correction) for S_1 and S_2 states, respectively. We further report *three higher-lying triplet states*, with energies again in very good agreement with the observed triplet bands. We suggest that most of the remaining bias in our DMC energies can be removed by *finite-temperature corrections*. Finally, we report *experimental high-lying singlet and triplet EEL bands in the 6–8 eV range*, outside of the common range of UV spectrometers. This provides the *most complete characterization of electronic structure of AB* to date by a joint experimental/theory study.

The EEL spectra reveal two close-lying states in the band around 4 eV, which has long been assigned to only one (S_2) state. The lower of these two states has a pronounced vibrational structure with a spacing of 0.145 ± 0.025 eV and peaks ($v = 1$) at 3.91 eV. The upper is structureless and peaks at 4.10 eV. The lower state is more pronounced in EEL spectra recorded with a low residual energy, indicating a "partly forbidden" nature. These findings are consistent with the observation of two distinct decay times across the "S_2-band" by Schultz *et al.*,[20] interpreted as due to partly overlapping S_2 and $S_{3,4}$ states. These findings are also consistent with the more recent calculations,[13,18–20] predicting three closely-lying states around this energy, one with a large oscillator strength (S_2), one with a small oscillator strength, and one forbidden (the latter two, $S_{3,4}$, are nearly degenerate and their ordering depends on model). The assignment of the experimental bands to these close-lying calculated states is not quite resolved—their ordering is not certain and it is puzzling why many theories predict the S_2 state slightly too high. We suggest that the latter problem could be due, at least in part, to the effect of finite temperature which lowers the experimental band maximum. We note that calculating the Franck-Condon profiles for the S_2, S_3 and S_4 states would be helpful in resolving the problem of ordering, since the observed bands have markedly different profiles.

Finally we expect that with advent of QMC force methods[50] fully dynamical QMC simulations on ground- and excited-state PESs of accuracy similar to the one achieved here for the single-point energies will become feasible. This will make a consistent QMC treatment of electronic and atomic structure possible and open up novel unconventional alternative routes to high-accuracy modeling of finite-temperature effects, conical intersections, statistical sampling of PESs, *etc*. Work along that line is now under way.

Acknowledgements

Financial support from APVV projects APVV-0091-07, LPP-0392-09 is acknowledged. This research was supported in

part also by ERDF OP R&D, Project CE meta-QUTE ITMS 26240120022, and *via* CE SAS QUTE. MA acknowledges support from project No. 200020-131962/1 of the Swiss National Science Foundation, of project SBF No. C07.0018 of the State Secretariat for Education and Research and of COST Action CM0601.

References

1 H. Rau, *Phtochromism: Molecules and Systems*, ed. H. Dürr and H. Bouas-Laurent, Elsevier, Amsterdam, 1990.
2 *Molecular Switches*, ed. B. L. Feringa, Wiley-VCH, Weinheim, 2001.
3 C. Zhang, M. H. Du, H. P. Cheng, X. G. Zhang, A. E. Roitberg and J. L. Krause, *Phys. Rev. Lett.*, 2004, **92**, 158301.
4 J.-Å. Andersson, R. Petterson and L. Tegnér, *J. Photochem.*, 1982, **20**, 17.
5 H. Rau, *Angew. Chem., Int. Ed. Engl.*, 1973, **12**, 224.
6 T. Nägele, R. Hoche, W. Zinth and J. Wachtveitl, *Chem. Phys. Lett.*, 1997, **272**, 489.
7 I. K. Lednev, T.-Q. Ye, R. E. Hester and J. N. Moore, *J. Phys. Chem.*, 1996, **100**, 13338.
8 A. W. Adamson, A. Vogler, H. Kunkely and R. J. Wachter, *J. Am. Chem. Soc.*, 1978, **100**, 1298.
9 A. Cembran, F. Bernardi, M. Garavelli, L. Gagliardi and G. Orlandi, *J. Am. Chem. Soc.*, 2004, **126**, 3234.
10 V. E. Shashoua, *J. Am. Chem. Soc.*, 1960, **82**, 5505.
11 S. Monti, E. Gardini, P. Bortolus and E. Amouyal, *Chem. Phys. Lett.*, 1981, **77**, 115.
12 L. Gagliardi, G. Orlandi, F. Bernardi, A. Cembran and M. Garavelli, *Theor. Chem. Acc.*, 2004, **111**, 363.
13 C. Hättig and K. Hald, *Phys. Chem. Chem. Phys.*, 2002, **4**, 2111.
14 C. Nonnenberg, H. Gaub and I. Frank, *ChemPhysChem*, 2006, **7**, 1455.
15 M. Böckmann, N. L. Doltsinis and D. Marx, *J. Phys. Chem. A*, 2010, **114**, 745.
16 R. Turanský, M. Konôpka, N. L. Doltsinis, I. Štich and D. Marx, *ChemPhysChem*, 2010, **11**, 345.
17 R. Turanský, M. Konôpka, N. L. Doltsinis, I. Štich and D. Marx, *Phys. Chem. Chem. Phys.*, 2010, **12**, 13922.
18 H. Fliegl, A. Köhn, C. Hättig and R. Ahlrichs, *J. Am. Chem. Soc.*, 2003, **125**, 9821.
19 I. Conti, M. Garavelli and G. Orlandi, *J. Am. Chem. Soc.*, 2008, **130**, 5216.
20 T. Schultz, J. Quenneville, B. Levine, A. Toniolo, T. J. Martínez, S. Lochbrunner, M. Schmitt, J. P. Shaffer, M. Z. Zgierski and A. Stolow, *J. Am. Chem. Soc.*, 2003, **125**, 8098.
21 A. Toniolo, C. Ciminelli, M. Persico and T. J. Martínez, *J. Chem. Phys.*, 2005, **123**, 234308.
22 T. Ishikawa, T. Noro and T. Shoda, *J. Chem. Phys.*, 2001, **115**, 7503.
23 L. Wang, W. Xu, C. Yi and X. Wang, *J. Mol. Graphics Modell.*, 2009, **27**, 792.
24 M. Dubecký, R. Derian, L. Mitas and I. Štich, *J. Chem. Phys.*, 2010, **133**, 244301.
25 W. M. C. Foulkes, L. Mitas, R. J. Needs and G. Rajagopal, *Rev. Mod. Phys.*, 2001, **73**, 33.
26 M. Bajdich and L. Mitas, *Acta Phys. Slovaca*, 2009, **59**, 81.
27 F. Schautz and C. Filippi, *J. Chem. Phys.*, 2004, **120**, 10931.
28 F. Schautz, F. Buda and C. Filippi, *J. Chem. Phys.*, 2004, **121**, 5836.
29 P. M. Zimmerman, J. Toulouse, Z. Zhang, C. B. Musgrave and C. J. Umrigar, *J. Chem. Phys.*, 2009, **131**, 124103.
30 T. Bouabça, N. B. Amor, D. Maynau and M. Caffarel, *J. Chem. Phys.*, 2009, **130**, 114107.
31 O. Valsson and C. Filippi, *J. Chem. Theory Comput.*, 2010, **6**, 1275.
32 C. Filippi, M. Zaccheddu and F. Buda, *J. Chem. Theory Comput.*, 2009, **5**, 2074.
33 R. Send, O. Valsson and C. Filippi, *J. Chem. Theory Comput.*, 2011, **7**, 444.
34 M. Allan, *J. Electron Spectrosc. Relat. Phenom.*, 1989, **48**, 219.
35 K. R. Asmis and M. Allan, *J. Chem. Phys.*, 1997, **106**, 7044.
36 I. Štich, *Acta Phys. Slovaca*, 2007, **57**, 1.
37 M. W. Schmidt, K. K. Baldridge, J. A. Boatz, S. T. Elbert, M. S. Gordon, J. H. Jensen, S. Koseki, N. Matsunaga, K. A. Nguyen and S. Su, *et al.*, *J. Comput. Chem.*, 1993, **14**, 1347.
38 S. Gordon and M. W. Schmidt, *Theory and Applications of Computational Chemistry: The First Forty Years*, ed. C. E. Dykstra, G. Frenking, K. S. Kim and G. E. Scuseria, Elsevier, Amsterdam, 2005, vol. 337, p. 1167.
39 L. Wagner, M. Bajdich and L. Mitas, *J. Comput. Phys.*, 2009, **228**, 3390, http://www.qwalk.org.
40 D. Marx and J. Hutter, *Modern Methods and Algorithms of Quantum Chemistry*, ed. J. Grotendorst, FZ Jülich, NIC, 2000, p. 301; for code see www.cpmd.org.
41 (*a*) A. D. Becke, *J. Chem. Phys.*, 1993, **98**, 5648; (*b*) P. J. Stephens, F. J. Delvin, C. F. Chabalowski and M. J. Frisch, *J. Phys. Chem.*, 1994, **98**, 11623.
42 C. W. Greeff and W. A. Lester, *J. Chem. Phys.*, 1998, **109**, 1607.
43 I. Ovcharenko, A. Aspuru-Guzik and W. A. Lester, *J. Chem. Phys.*, 2001, **114**, 7790.
44 T. H. Dunning, *J. Chem. Phys.*, 1989, **90**, 1007.
45 T. Tsuji, H. Takashima, H. Takeuchi, T. Egawa and S. Konaka, *J. Phys. Chem. A*, 2001, **105**, 9345.
46 K. E. Schmidt and J. W. Moskowitz, *J. Chem. Phys.*, 1990, **93**, 4172.
47 C. J. Umrigar and C. Filippi, *Phys. Rev. Lett.*, 2005, **94**, 150201.
48 H. Rau and G. Kortüm, *Ber. Bunsen-Ges.*, 1967, **71**, 664.
49 J. Bao and P. M. Weber, *J. Am. Chem. Soc.*, 2011, **133**, 4164.
50 C. Filippi and C. J. Umrigar, *Phys. Rev. B: Condens. Matter*, 2000, **61**, R16291.